was observed for MDC1. The incidence of ABRA1 methylation was relatively high in pCR cases (6/20 cases: 30%) than that in poor responders (1/19 cases: 5.3%), although there was no statistical significance. When examining all 16 genes together, we could not detect any association between aberrant DNA methylation status and tumor response to the chemotherapy in either LBC or TNBC. We expected higher incidence of methylation in pCR cases than in poor responders. However, interestingly, significantly higher incidences of methylation were observed in poor responders than in pCR in TNBC for RNF8 and ATM. The biological background underlying this phenomenon is currently unclear. Overall, the levels of methylation of the new HR genes investigated in the current study were not as significant as that of BRCA1, reaffirming the importance of BRCA1 in breast cancer pathogenesis. Nonetheless, we found that a combination of 5 genes, BRCA1, BRCA2, MDC1, ABRA1 and PALB2, possessed the greatest sensitivity, specificity and AUC associated with pCR in TNBC. Hypermethylation of these genes could be a candidate biomarker of breast cancer chemosensitivity and warrants validation in separate data sets.

HER2-negative LBC has been classified as Luminal A and Luminal B subtypes according to a low index and high Ki-67 index, respectively. In general, Luminal B breast cancer is more sensitive to chemotherapy than Luminal A. Therefore, we analyzed the index to clarify whether it associates with pCR. However, pCR cases exhibited even lower levels of Ki-67 when compared with SD or poor-responder cases in both LBC and TNBC, suggesting that a high Ki-67 index is not an efficient marker for chemosensitivity.

In conclusion, this is the first study to quantitatively analyze the aberrant DNA methylation status of HR genes, including BRCA1 and BRCA2, in breast cancer tissues for their association with tumor subtypes and tumor response to chemotherapy. The aberrant DNA methylation status of most of the HR genes studied was not significantly associated with TNBC subtype or chemosensitivity. However, hypermethylation of BRCA1 and RNF8 is associated with TNBC subtype and may impact chemosensitivity. Contrary to our expectation, no severe methylation was observed in LBC with pCR, with the exception of one case that exhibited 100% methylation of PALB2. Because the current study includes only a part of the essential HR genes, future work may be required to identify the possibly missing key HR gene(s) critical for the chemosensitivity.

Experimental procedures

Patients and biopsy specimens

Of the 384 patients with primary invasive breast cancer who underwent neoadjuvant chemotherapy at the Division of Breast and Endocrine Surgery, St. Marianna University School of Medicine, Japan, from August 2007 to August 2010, fifteen sequential cases each of either LBC with pCR, LBC with nonresponding stable disease (SD), TNBC with pCR, or TNBC with poor response were selected for examination. Because the TNBC cases included only 1 case of progressive disease (PD) and 3 cases of SD, an additional 11 cases with partial responses that exhibited the smallest rate of regression in the partial-response cases were analyzed to adjust the total number in the group to 15 cases. HER2-positive patients were excluded because they had been treated with neoadjuvant chemotherapy combined with trastuzumab. Tumor specimens were obtained by core needle biopsy prior to starting therapy for the purpose of diagnosis, and formalin-fixed, paraffin-embedded (FFPE) specimens were stored. Excess specimen samples were analyzed in accordance with an approved Institutional Review Board application of the St. Marianna University School of Medicine (registration number 1865).

Neoadjuvant chemotherapy

The chemotherapy regimen consisted of four 21-day cycles of FEC (5-Fu: 500 mg/m^2, epirubicin: 100 mg/m^2, cyclophosphamide: 500 mg/m^2 on day 1) or EC (epirubicin: 80–90 mg/m^2, cyclophosphamide: 600 mg/m^2 on day 1) followed by four 21-day cycles of DOC (docetaxel: 75 mg/m^2 on day 1), except for two patients in the TNBC-poor-responder group as described in Table 1.

Response evaluation

The pathological response of the tumor to the neoadjuvant chemotherapy was evaluated with hematoxylin-eosin-stained specimens obtained during the primary surgeries. The absence of invasive cancer in the primary lesion following the chemotherapy was defined as pCR. The clinical response was evaluated using the Response Evaluation Criteria in Solid Tumors (RECIST) criteria.

Gene and primer selection

The HR genes implicated in breast cancer susceptibility were included in the study. In addition, genes evidently involved in and critically functioning in HR (Ciccia & Elledge 2010) that contain appropriate CpG islands around their promoter region were selected as candidates. A flow chart of the process for gene selection is shown in Fig. S2. The sequence and the position of each pair of primers are shown in Table S3 and Fig. S3.

DNA extraction

FFPE specimens were cut in 10 μm sections and subjected to laser-capture microdissection to isolate cancer cells using the PALM Microbeam (Carl Zeiss, Oberkohen, Germany). DNA was extracted using the standard phenol–chloroform method from breast, colorectal and gastric cancer cell lines and microdissected breast cancer tissues.

Bisulfite-pyrosequencing

Bisulfite treatment of gDNA, subsequent polymerase chain reaction (PCR) and pyrosequencing have been performed as described previously (Watanabe *et al.* 2009). All of the primers and PCR conditions used for amplifying CpG island DNA fragments of candidate methylation HR genes are listed in Table S3.

Immunohistochemical analysis

The status of hormone receptors HER2 and Ki-67/MIB-1 was determined by standard immunohistochemical analysis with DaKo Envision system (Dako, Denmark) and fluorescence *in situ* hybridization (FISH). The cutoff value for ERα -negative and PR-negative cases was 10%, and tumors with less than 10% expression were considered negative. For HER2 status, tumors that were immunohistochemically scored as (0+) (1+), or (2+) and were FISH negative were regarded as HER2 negative (no amplification). In the HER2-negative cases analyzed in the study, ERα -positive and/or PR-positive cases were defined as LBC, and ERα -negative and PR-negative cases were defined as TNBC.

Statistical analysis

All statistical analyses were performed using SPSS for Windows, version 12 (SPSS, Inc., Chicago, IL), and PRISM software for Windows, version 4 (GraphPad Prism, Inc., San Diego, CA). The methylation level (%) was analyzed as a continuous variable for the comparison of each gene with the sample's clinicopathologic features; mean and 95% confidence intervals (CIs) were calculated. Associations between continuous variables or the levels of DNA methylation and clinicopathologic variables were evaluated using analysis of variance (ANOVA) and Student's *t*-test. In parallel, we computed the median DNA methylation value and range for each sample, and we defined the receiver operating characteristic (ROC) curve (AUC) in SPSS software. *Z*-score analysis was used to normalize the methylation levels of several genes in each sample. The *Z*-score for each gene was calculated as follows: *Z*-score = (methylation level of each sample − mean value of methylation level)/standard deviation of methylation level. In this analysis, a *Z*-score greater than 0 means that the methylation level is greater than the mean value for the population. All reported P values were two-sided, and $P < 0.05$ was considered statistically significant.

Acknowledgements

We thank members in the Division of Breast and Endocrine Surgery for support in analyses of clinical data and Mrs. Shigeko Ohnuma and Mrs. Makiko Takahashi for technical support for immunohistochemical experiments. This study was supported by grants-in-aid from the Ministry of Education, Science, Sports, Culture and Technology of Japan, the Ministry of Health, Labour and Welfare of Japan, and the Japan Private School Promotion Foundation.

References

Alvarez, S., Diaz-Uriarte, R., Osorio, A., Barroso, A., Melchor, L., Paz, M.F., Honrado, E., Rodríguez, R., Urioste, M., Valle, L., Díez, O., Cigudosa, J.C., Dopazo, J., Esteller, M. & Benitez, J. (2005) A predictor based on the somatic genomic changes of the BRCA1/BRCA2 breast cancer tumors identifies the non-BRCA1/BRCA2 tumors with BRCA1 promoter hypermethylation. *Clin. Cancer Res.* **11**, 1146–1153.

Audeh, M.W., Carmichael, J., Penson, R.T., Friedlander, M., Powell, B., Bell-McGuinn, K.M., Scott, C., Weitzel, J.N., Oaknin, A., Loman, N., Lu, K., Schmutzler, R.K., Matulonis, U., Wickens, M. & Tutt, A. (2010) Oral poly(ADP-ribose) polymerase inhibitor olaparib in patients with BRCA1 or BRCA2 mutations and recurrent ovarian cancer: A proof-of-concept trial. *Lancet* **376**, 245–251.

Branham, M.T., Marzese, D.M., Laurito, S.R., Gago, F.E., Orozco, J.I., Tello, O.M., Vargas-Roig, L.M. & Roqué, M. (2012) Methylation profile of triple-negative breast carcinomas. *Oncogenesis* **1**, e17.

Byrski, T., Huzarski, T., Dent, R., Gronwald, J., Zuziak, D., Cybulski, C., Kladny, J., Gorski, B., Lubinski, J. & Narod, S.A. (2009) Response to neoadjuvant therapy with cisplatin in BRCA1-positive breast cancer patients. *Breast Cancer Res. Treat.* **115**, 359–363.

Cantor, S.B., Bell, D.W., Ganesan, S., Kass, E.M., Drapkin, R., Grossman, S., Wahrer, D.C., Sgroi, D.C., Lane, W.S., Haber, D.A. & Livingston, D.M. (2001) BACH1, a novel helicase-like protein, interacts directly with BRCA1 and contributes to its DNA repair function. *Cell* **105**, 149–160.

Catteau, A., Harris, W.H., Xu, C.F. & Solomon, E. (1999) Methylation of the BRCA1 promoter region in sporadic breast and ovarian cancer: correlation with disease characteristics. *Oncogene* **18**, 1957–1965.

Cerne, J.Z., Zong, L., Jelinek, J., Hilsenbeck, S.G., Wang, T., Oesterreich, S. & McGuire, S.E. (2012) BRCA1 promoter methylation status does not predict response to tamoxifen in sporadic breast cancer patients. *Breast Cancer Res. Treat.* **135**, 135–143.

Chen, Y., Zhou, J., Xu, Y., Li, Z., Wen, X., Yao, L., Xie, Y. & Deng, D. (2009) BRCA1 promoter methylation associated with poor survival in Chinese patients with sporadic breast cancer. *Cancer Sci.* **100**, 1663–1667.

Ciccia, A. & Elledge, S.J. (2010) The DNA damage response: making it safe to play with knives. *Mol. Cell* **40**, 179–204.

Collins, N., Wooster, R. & Stratton, M.R. (1997) Absence of methylation of CpG dinucleotides within the promoter of the breast cancer susceptibility gene BRCA2 in normal tissues and in breast and ovarian cancers. *Br. J. Cancer* **76**, 1150–1156.

Cucer, N., Taheri, S., Ok, E. & Ozkul, Y. (2008) Methylation status of CpG islands at sites -59 to +96 in exon 1 of the BRCA2 gene varies in mammary tissue among women with sporadic breast cancer. *J. Genet.* **87**, 155–158.

Dobrovic, A. & Simpfendorfer, D. (1997) Advances in Brief Methylation of the BRCAJ Gene in Sporadic Breast Cancer. *Cancer Res.* **57**, 3347–3350.

Esteller, M., Fraga, M.F., Guo, M. *et al.* (2001) DNA methylation patterns in hereditary human cancers mimic sporadic tumorigenesis. *Hum. Mol. Genet.* **10**, 3001–3007.

Esteller, M., Silva, J.M., Dominguez, G., Bonilla, F., Matias-Guiu, X., Lerma, E., Bussaglia, E., Prat, J., Harkes, I.C., Repasky, E.A., Gabrielson, E., Schutte, M., Baylin, S.B. & Herman, J.G. (2000) Promoter hypermethylation and BRCA1 inactivation in sporadic breast and ovarian tumors. *J. Natl. Cancer Inst.* **92**, 564–569.

Heikkinen, K., Rapakko, K., Karppinen, S.M., Erkko, H., Knuutila, S., Lundán, T., Mannermaa, A., Børresen-Dale, A.L., Borg, A., Barkardottir, R.B., Petrini, J. & Winqvist, R. (2006) RAD50 and NBS1 are breast cancer susceptibility genes associated with genomic instability. *Carcinogenesis* **27**, 1593–1599.

Hsu, N.C., Huang, Y.F., Yokoyama, K.K., Chu, P.Y., Chen, F.M. & Hou, M.F. (2013) Methylation of BRCA1 Promoter Region Is Associated with Unfavorable Prognosis in Women with Early-Stage Breast Cancer. *PLoS ONE* **8**, e56256.

Jönsson, G., Staaf, J., Vallon-Christersson, J. *et al.* (2010) Genomic subtypes of breast cancer identified by array-comparative genomic hybridization display distinct molecular and clinical characteristics. *Breast Cancer Res.* **12**, R42.

Litman, R., Peng, M., Jin, Z., Zhang, F., Zhang, J., Powell, S., Andreassen, P.R. & Cantor, S.B. (2005) BACH1 is critical for homologous recombination and appears to be the Fanconi anemia gene product FANCJ. *Cancer Cell* **8**, 255–265.

Livingston, D.M. & Silver, D.P. (2008) Cancer: crossing over to drug resistance. *Nature* **451**, 1066–1067.

Magdinier, F., Ribieras, S., Lenoir, G.M., Frappart, L. & Dante, R. (1998) Down-regulation of BRCA1 in human sporadic breast cancer; analysis of DNA methylation patterns of the putative promoter region. *Oncogene* **17**, 3169–3176.

Margeli, M., Cirauqui, B., Castella, E., Tapia, G., Costa, C., Gimenez-Capitan, A., Barnadas, A., Sanchez Ronco, M., Benlloch, S., Taron, M. & Rosell, R. (2010) The Prognostic Value of BRCA1 mRNA Expression Levels Following Neoadjuvant Chemotherapy in Breast Cancer. *PLoS ONE* **5**, e9499.

Matros, E., Wang, Z.C., Lodeiro, G., Miron, A., Iglehart, J.D. & Richardson, A.L. (2005) BRCA1 promoter methylation in sporadic breast tumors: relationship to gene expression profiles. *Breast Cancer Res. Treat.* **91**, 179–186.

Meindl, A., Hellebrand, H., Wiek, C. *et al.* (2010) Germline mutations in breast and ovarian cancer pedigrees establish RAD51C as a human cancer susceptibility gene. *Nat. Genet.* **42**, 410–414.

Moelans, C.B., Verschuur-Maes, A.H.J. & Van Diest, P.J. (2011) Frequent promoter hypermethylation of BRCA2, CDH13, MSH6, PAX5, PAX6 and WT1 in ductal carcinoma *in situ* and invasive breast cancer. *J. Pathol.* **225**, 222–231.

Moskwa, P., Buffa, F.M., Pan, Y., Panchakshari, R., Gottipati, P., Muschel, R.J., Beech, J., Kulshrestha, R., Abdelmohsen, K., Weinstock, D.M., Gorospe, M., Harris, A.L., Helleday, T. & Chowdhury, D. (2011) miR-182-mediated downregulation of BRCA1 impacts DNA repair and sensitivity to PARP inhibitors. *Mol. Cell* **41**, 210–220.

Niwa, Y., Oyama, T. & Nakajima, T. (2000) BRCA1 expression status in relation to DNA methylation of the BRCA1 promoter region in sporadic breast cancers. *Jpn. J. Cancer Res.* **91**, 519–526.

Ohta, T., Sato, K. & Wu, W. (2011) The BRCA1 ubiquitin ligase and homologous recombination repair. *FEBS Lett.* **585**, 2836–2844.

Potapova, A., Hoffman, A.M., Godwin, A.K., Al-Saleem, T. & Cairns, P. (2008) Promoter hypermethylation of the PALB2 susceptibility gene in inherited and sporadic breast and ovarian cancer. *Cancer Res.* **68**, 998–1002.

Rahman, N., Seal, S., Thompson, D. *et al.* (2007) PALB2, which encodes a BRCA2-interacting protein, is a breast cancer susceptibility gene. *Nat. Genet.* **39**, 165–167.

Renwick, A., Thompson, D., Seal, S. *et al.* (2006) ATM mutations that cause ataxia-telangiectasia are breast cancer susceptibility alleles. *Nat. Genet.* **38**, 873–875.

Rice, J.C., Ozcelik, H., Maxeiner, P., Andrulis, I. & Futscher, B.W. (2000) Methylation of the BRCA1 promoter is associated with decreased BRCA1 mRNA levels in clinical breast cancer specimens. *Carcinogenesis* **21**, 1761–1765.

Sorlie, T., Tibshirani, R., Parker, J. *et al.* (2003) Repeated observation of breast tumor subtypes in independent gene expression data sets. *Proc. Natl Acad. Sci. USA* **100**, 8418–8423.

Steffen, J., Varon, R., Mosor, M. *et al.* (2004) Increased cancer risk of heterozygotes with NBS1 germline mutations in Poland. International journal of cancer. *Int. J. Cancer* **111**, 67–71.

Treilleux, I., Chapot, B., Goddard, S., Pisani, P., Angèle, S. & Hall, J. (2007) The molecular causes of low ATM protein expression in breast carcinoma; promoter methylation and levels of the catalytic subunit of DNA-dependent protein kinase. *Histopathol* **51**, 63–69.

Turner, N.C., Reis-Filho, J.S., Russell, A.M., Springall, R.J., Ryder, K., Steele, D., Savage, K., Gillett, C.E., Schmitt, F.C., Ashworth, A. & Tutt, A.N. (2007) BRCA1 dysfunction in sporadic basal-like breast cancer. *Oncogene* **26**, 2126–2132.

Tutt, A., Robson, M., Garber, J.E., Domchek, S.M., Audeh, M.W., Weitzel, J.N., Friedlander, M., Arun, B., Loman, N., Schmutzler, R.K., Wardley, A., Mitchell, G., Earl, H., Wickens, M. & Carmichael, J. (2010) Oral poly(ADP-

ribose) polymerase inhibitor olaparib in patients with BRCA1 or BRCA2 mutations and advanced breast cancer: a proof-of-concept trial. *Lancet* **376**, 235–244.

Vo, Q.N., Kim, W.J., Cvitanovic, L., Boudreau, D.A., Ginzinger, D.G. & Brown, K.D. (2004) The ATM gene is a target for epigenetic silencing in locally advanced breast cancer. *Oncogene* **23**, 9432–9437.

Watanabe, Y., Kim, H.S., Castoro, R.J., Chung, W., Estecio, M.R., Kondo, K., Guo, Y., Ahmed, S.S., Toyota, M., Itoh, F., Suk, K.T., Cho, M.Y., Shen, L., Jelinek, J. & Issa, J.P. (2009) Sensitive and specific detection of early gastric cancer with DNA methylation analysis of gastric washes. *Gastroenterology* **136**, 2149–2158.

Wei, M., Grushko, T.A., Dignam, J., Hagos, F., Nanda, R., Sveen, L., Xu, J., Fackenthal, J., Tretiakova, M., Das, S. & Olopade, O.I. (2005) BRCA1 promoter methylation in sporadic breast cancer is associated with reduced BRCA1 copy number and chromosome 17 aneusomy. *Cancer Res.* **65**, 10692–10699.

Wei, M., Xu, J., Dignam, J., Nanda, R., Sveen, L., Fackenthal, J., Grushko, T.A. & Olopade, O.I. (2008) Estrogen receptor alpha, BRCA1, and FANCF promoter methylation occur in distinct subsets of sporadic breast cancers. *Breast Cancer Res. Treat.* **111**, 113–120.

Xu, X., Gammon, M.D., Zhang, Y., Bestor, T.H., Zeisel, S.H., Wetmur, J.G., Wallenstein, S., Bradshaw, P.T., Garbowski, G., Teitelbaum, S.L., Neugut, A.I., Santella, R.M. & Chen, J. (2009) BRCA1 promoter methylation is associated with increased mortality among women with breast cancer. *Breast Cancer Res. Treat.* **115**, 397–404.

Xu, Y., Diao, L., Chen, Y., Liu, Y., Wang, C., Ouyang, T., Li, J., Wang, T., Fan, Z., Fan, T., Lin, B., Deng, D., Narod, S.A. & Xie, Y. (2013) Promoter methylation of BRCA1 in triple-negative breast cancer predicts sensitivity to adjuvant chemotherapy. *Annals Oncol.* **24**, 1498–1505.

Zhang, F., Ma, J., Wu, J., Ye, L., Cai, H., Xia, B. & Yu, X. (2009) PALB2 links BRCA1 and BRCA2 in the DNA-damage response. *Curr. Biol.* **19**, 524–529.

Received: 5 August 2013
Accepted: 6 September 2013

Supporting Information

Additional Supporting Information may be found in the online version of this article at the publisher's web site:

Table S1 Aberrant DNA methylation status of HR genes in cancer cell lines

Table S2 Aberrant DNA methylation status of HR genes in breast cancer tissues

Table S3 Sequence and the position of primers used in the study

Figure S1 An example pyro-gram data for the sequence of bisulfite-treated DNA in 6 final candidate genes (BRCA1, BRCA2, BARD1, MDC1, ABRA1 and PALB2).

Figure S2 Summary of the process for selection of the genes to be addressed in the current study.

Figure S3 The sequence and position of the primers used in the study. Black bars with arrows indicate the coding region of HR genes.

Molecular Cell
Article

Fine-Tuning of DNA Damage-Dependent Ubiquitination by OTUB2 Supports the DNA Repair Pathway Choice

Kiyoko Kato,[1,5] Kazuhiro Nakajima,[1,5] Ayako Ui,[2] Yuri Muto-Terao,[3] Hideaki Ogiwara,[4] and Shinichiro Nakada[1,*]
[1]Department of Bioregulation and Cellular Response, Graduate School of Medicine, Osaka University, 2-2Yamadaoka, Suita, Osaka, 565-0871, Japan
[2]Division of Dynamic Proteome in Aging and Cancer, Institute of Development, Aging and Cancer, Tohoku University, 4-1 Seiryomachi, Aoba-ku, Sendai, Miyagi, 980-8575, Japan
[3]Center for Medical Research and Education, Graduate School of Medicine, Osaka University, 2-2 Yamadaoka, Suita, Osaka, 565-0871, Japan
[4]Division of Genome Biology, National Cancer Center Research Institute, 5-1-1 Tsukiji, Chuo-ku, 104-0045, Tokyo, Japan
[5]These authors contributed equally to this work
*Correspondence: snakada@bcr.med.osaka-u.ac.jp
http://dx.doi.org/10.1016/j.molcel.2014.01.030

SUMMARY

DNA double-strand breaks (DSBs) are deleterious lesions that lead to genetic mutations and cell death. Protein ubiquitination mediated by the E3 ubiquitin ligase RNF8 within the regions surrounding DSBs recruits DNA DSB response (DDR) factors and induces chromatin remodeling, which supports cell survival after DNA damage. Nevertheless, the impact of RNF8-mediated ubiquitination on DNA repair remains to be elucidated. Here, we report that depletion of the deubiquitinating enzyme OTUB2 enhances RNF8-mediated ubiquitination in an early phase of the DDR and promotes faster DSB repair but suppresses homologous recombination. The rapid ubiquitination results in accelerated accumulation of 53BP1 and RAP80 at DSBs, which in turn protects DSB ends from resection in OTUB2-depleted cells. Mechanistically, OTUB2 suppresses RNF8-mediated L3MBTL1 ubiquitination and Lys 63-linked ubiquitin chain formation in a deubiquitinating activity-dependent manner. Thus, OTUB2 fine-tunes the speed of DSB-induced ubiquitination so that the appropriate DNA repair pathway is chosen.

INTRODUCTION

DNA double-strand break (DSB) response (DDR) signaling is regulated by posttranslational modifications. The first step of this signaling pathway involves the ATM-dependent phosphorylation of various proteins, including histone H2AX and the mediator protein MDC1 (Al-Hakim et al., 2010). The phosphorylation of these proteins promotes the recruitment of E3 ubiquitin ligases to DSBs, and the signaling then becomes controlled by ubiquitination.

The E3 ubiquitin ligase RNF8 initiates DNA damage-dependent ubiquitination (Huen et al., 2007; Kolas et al., 2007; Mailand et al., 2007) and recruits RNF168, an ubiquitin interaction motif-containing E3 ubiquitin ligase, to DSBs (Doil et al., 2009; Stewart et al., 2009). RNF168 ubiquitinates Lys 13-15 on histones H2A and H2AX (Mattiroli et al., 2012). These E3s and their cognate E2-conjugating enzyme UBC13 (Zhao et al., 2007) also elongate the Lys 63-linked ubiquitin chains within the region surrounding the DSBs. The Lys 63-linked ubiquitin chains act as a scaffold for the retention of the Lys 63-linked ubiquitin chain-binding protein RAP80 at DSBs (Kim et al., 2007; Sobhian et al., 2007; Wang et al., 2007). Recent studies have revealed that the polycomb molecule L3MBTL1 (Acs et al., 2011) and the lysine demethylase JMJD2A (Mallette et al., 2012) are also substrates of RNF8. L3MBTL1 and JMJD2A interact with Lys 20 dimethylated histone H4 (H4K20me2) through the MBT domains and the tandem TUDOR domain, respectively (Kim et al., 2006; Mallette et al., 2012). Upon DNA damage, the ubiquitination of L3MBTL1 and JMJD2A induces the removal of L3MBTL1 and JMJD2A from damaged chromatin and exposes H4K20me2, which is then bound by the tandem TUDOR domain-containing DDR protein 53BP1 (Acs et al., 2011; Mallette et al., 2012). 53BP1 also possesses a ubiquitination-dependent recruitment (UDR) motif, which enables 53BP1 to interact tightly with nucleosomes containing both H4K20me2 and RNF168-dependent ubiquitinated histone H2A even in the presence of L3MBTL1 and JMJD2A (Fradet-Turcotte et al., 2013).

These RNF8/RNF168-dependent ubiquitination events are opposed by several deubiquitinating enzymes (DUBs). A Lys 63-linked ubiquitin-specific DUB, BRCC36, localizes to DSBs as part of the RAP80-containing multiprotein complex and deubiquitinates ubiquitin chains at DSBs (Shao et al., 2009). POH1 is another Lys 63 linkage-specific DUB that has been suggested to negatively regulate the accumulation of 53BP1 at DSBs (Butler et al., 2012). USP3 and USP16 remove ubiquitin from histone H2A during the DDR (Doil et al., 2009; Shanbhag et al., 2010). The otubain family DUB OTUB1 negatively regulates DSB-dependent ubiquitination differently than these DUBs. OTUB1 interacts with UBC13 (UBE2N) and the UBE2D/UBE2E

family E2 ubiquitin-conjugating enzymes and inhibits their E2 activities in a DUB activity-independent manner (Nakada et al., 2010; Sato et al., 2012; Wiener et al., 2012). Thus, DUBs have separate roles in the DDR, such as removing unnecessary ubiquitin after DNA repair and setting a threshold for ubiquitination. Because many substrates are ubiquitinated during the DDR, other DUBs are expected to contribute to the regulation of the DDR.

DSBs are repaired by the error-free homologous recombination (HR) pathway and the other pathways including nonhomologous end joining (NHEJ), alternative NHEJ, and single-strand annealing, i.e., non-HR repair pathway (Goodarzi and Jeggo, 2013). During the first step of HR, DSB edges are resected to form 3′ overhangs. The single-stranded DNA is rapidly coated with RPA, which is subsequently displaced by RAD51. The RAD51-DNA filament invades the homologous DNA on the identical sister chromatid, and the damaged DNA is then repaired in a DNA synthesis-dependent manner. In contrast, non-HR repair eliminates DSB by direct ligation of the ends of the DSB with minor processing (Symington and Gautier, 2011). The choice of an inappropriate repair pathway can lead to gene mutations and chromosomal translocations (Chapman et al., 2012). Therefore, one important question regarding DSB repair has been how cells choose the appropriate repair method. Recently, several groups have revealed that RIF1, a 53BP1 binding partner, inhibits DNA end resection and leads to cells choosing NHEJ over HR (Chapman et al., 2013; Di Virgilio et al., 2013; Escribano-Díaz et al., 2013; Zimmermann et al., 2013). Other groups have reported that RAP80 inhibits BRCA1-dependent excessive DNA end resection and hyperrecombination (Coleman and Greenberg, 2011; Hu et al., 2011). These HR-suppressing proteins accumulate at DSBs in an RNF8/RNF168-mediated ubiquitination-dependent manner, suggesting that RNF8/RNF168-mediated ubiquitination supports the DNA repair pathway choice.

In this study, we sought to analyze the impact of enhanced RNF8-dependent ubiquitination on the choice of DNA repair pathway. Using data from a DUB-specific small interfering RNA (siRNA) library screen, we identified OTUB2 as a suppressor of excessive ubiquitination in an early phase of the DDR. In contrast to OTUB1, OTUB2 suppresses ubiquitination in a DUB activity-dependent manner. Rapid DNA damage-dependent ubiquitination in OTUB2-depleted cells led to the enhanced recruitment of 53BP1 and RAP80 to DSBs and accelerated total DSB repair in an early phase of the DDR. In contrast, assembly of RPA and RAD51 at DSBs and HR were suppressed in OTUB2-depleted cells. These data indicate that non-HR pathway is preferentially selected in cells where RNF8-dependent ubiquitination is hyperactivated by OTUB2 depletion.

RESULTS

OTUB2 Inhibits RNF8-Dependent Ubiquitination

DSB repair process starts quickly after the generation of DSBs, suggesting that the DNA repair pathway is selected in a very early phase of DDR. We expected that efficiency of RNF8/RNF168-dependent ubiquitination in an early phase of DDR affect the choice of repair pathway. Accordingly, we screened an siRNA library of human DUBs to identify DUBs that, when depleted, enhanced the accumulation of RAP80 at DSBs soon after generation of the DSB. U2OS cells were transfected with pools of siRNAs, treated with the radiomimetic drug neocarzinostatin (NCS) for 5 min and subsequently processed for RAP80 immunofluorescence staining. Images were taken using an automated microscope, and the RAP80 focal intensity was then analyzed. Among the positive hits (in which siRNA transfection enhanced RAP80 foci) (Figures 1A and 1B), we focused on OTUB2 because our previous data implicated OTUB2 in the DDR. In our previous work, overexpression of OTUB2 did not inhibit ionizing radiation-induced 53BP1 foci formation as efficiently as OTUB1. However, its inhibitory effect was higher than that of an OTUB1 N-terminal deletion mutant that does not inhibit the E2 activity of UBC13 (Nakada et al., 2010).

To re-examine the ability of OTUB2 to inhibit 53BP1 foci formation, HeLa cells were transiently transfected with Flag-OTUB2 expression vectors, treated with NCS, and then subjected to Flag and 53BP1 immunofluorescence staining 1 hr post-NCS treatment. Flag-OTUB1 wild-type and the F133A/F138A/M211A (OTUB1^{AAA}) mutant, which does not interact with UBC13, were used as positive and negative controls, respectively (Nakada et al., 2010; Sato et al., 2012). When we analyzed cells with mild Flag-OTUB2 expression (Figures 1C and S1A), we found that OTUB2 did not inhibit formation of 53BP1 foci as strongly as did OTUB1, but it did inhibit 53BP1 foci formation more strongly than did the OTUB1^{AAA} mutant. However, when we analyzed cells with strong Flag-OTUB2 expression, we found that OTUB2 almost completely suppressed NCS-induced 53BP1 foci formation (Figures 1D and 1E). In contrast, the OTUB2^{C51S} mutant, which had very weak DUB activity, did not show the same inhibitory effect. Both OTUB1 and the catalytically inactive OTUB1^{C91S} mutant completely suppressed accumulation of 53BP1 at DSBs. These data were also confirmed by automated image acquisition and analysis using imaging software (Figure S1B). In addition, similar data were obtained using U2OS cells (Figure S2A), indicating that the function of OTUB2 does not depend on cell type.

The overexpression of OTUB2, which affects only a small fraction of the total amount of ubiquitinated protein and the free ubiquitin pool (Figure S1C), also suppressed NCS-induced ubiquitin conjugation, as detected using the FK2 antibody, in a DUB activity-dependent manner (Figures 2A and 2B). Although foci of Flag-OTUB2 were not detected after NCS treatment, a small amount of EGFP-OTUB2 colocalized with γH2AX at micro-laser-induced DSBs (Figure S1D). These data indicate that the mechanism by which OTUB2 inhibits the DDR is through its deubiquitination activity, which is different from that of OTUB1.

Next, we sought to pinpoint the step of DDR signaling that is sensitive to the DUB activity of OTUB2. We found that NCS-induced formation of RAP80, BRCA1, and RNF168 foci was almost completely suppressed by the overexpression of OTUB2 but not the OTUB2^{C51S} mutant (Figures 2C–2F, S2C, and S2D). In contrast, the overexpression of OTUB2 did not affect foci formation of γH2AX, MDC1, or EGFP-tagged RNF8^{C403S}; we utilized the catalytically inactive mutant RNF8^{C403S} (Mailand et al., 2007) to avoid inducing excessive ubiquitination by overexpressing active RNF8 (Figures 2G, 2H and S2E–S2H). Because the accumulation of RNF168 at DSBs

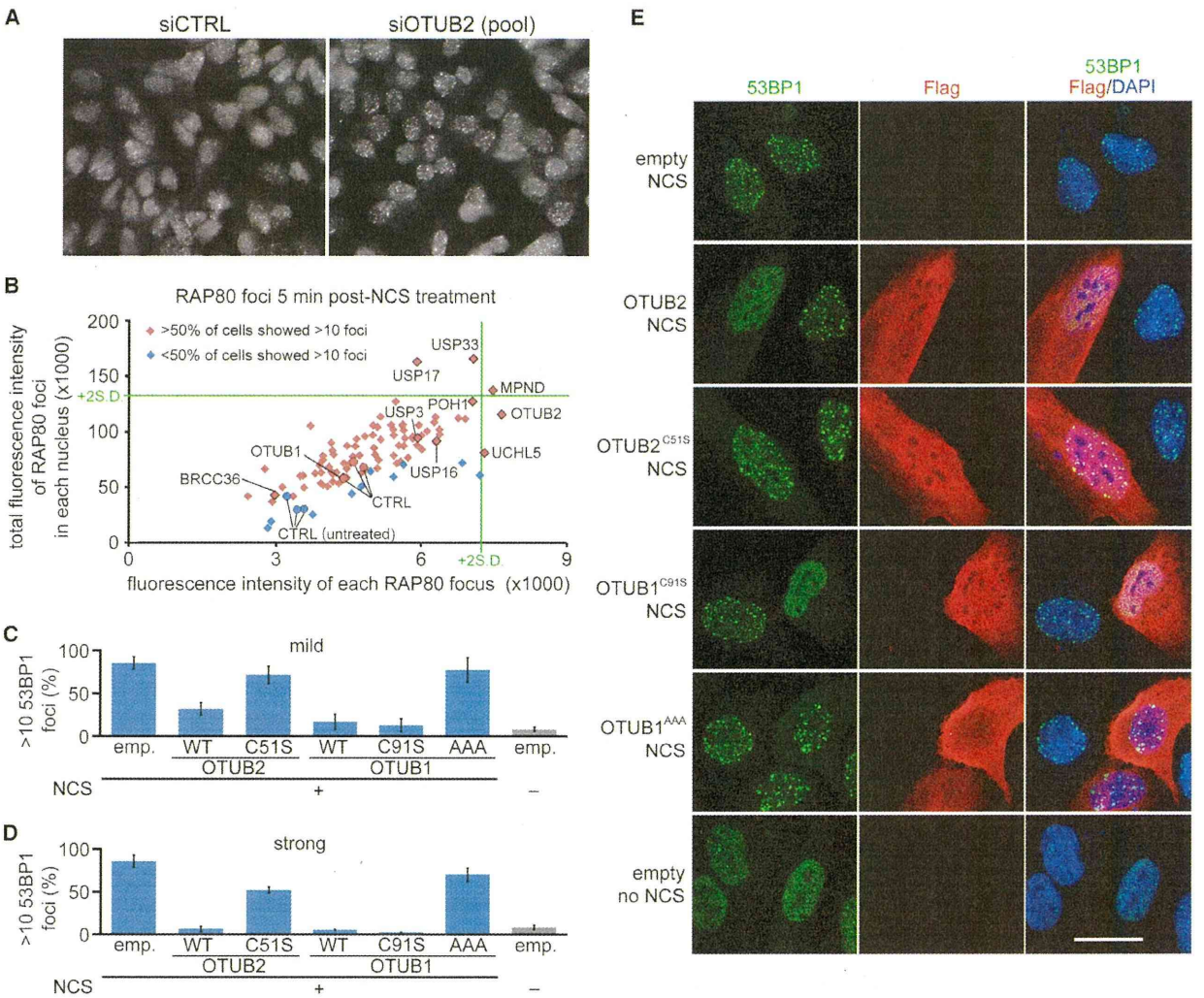

Figure 1. Analysis of siRNA Screen Data

(A) siRNAs from the siRNA library for human deubiquitinating enzymes were individually transfected into U2OS cells. These cells were treated with 5 ng/mL NCS and processed for RAP80 immunofluorescence staining 5 min after NCS treatment. Immunofluorescent images were obtained using an automated microscope, and the intensities of RAP80 foci were analyzed. Representative images from the screen are shown. Objective, 40×.

(B) Analyzed data from the screen. y axis: Total fluorescence intensity of RAP80 foci in each nucleus. x axis: Fluorescence intensity of each RAP80 focus. Three different nontargeting siRNAs were used as controls (CTRL).

(C and D) Quantification of cells with 53BP1 foci. HeLa cells transfected with the indicated Flag-OTUB2 or Flag-OTUB1 expression plasmids were processed for 53BP1 and Flag immunofluorescence staining 1 hr after 5 ng/mL NCS treatment. The percentage of cells containing >10 53BP1 foci are shown. A total of 100 cells from the Flag-OTUB2- or OTUB1-transfected cultures with mild (C) or strong (D) fusion protein expression or 100 cells from the control cultures transfected with the Flag-empty plasmid were analyzed from each sample. Data are presented as the mean ± SD of three independent experiments. emp., empty plasmid.

(E) Representative images of the immunofluorescence staining in (D) are shown. DNA was counterstained with DAPI. Scale bar, 25 μm. See also Figure S1.

requires the E3 ubiquitin ligase activity of RNF8 and the accumulation of 53BP1, RAP80, and BRCA1 requires recruitment of RNF168 to DSBs (Doil et al., 2009; Stewart et al., 2009), we suspect that OTUB2 inhibits RNF8-dependent ubiquitination.

OTUB2 Depletion Enhances the Accumulation of RAP80 and 53BP1 at DSBs

To analyze the physiological function of OTUB2, we monitored ubiquitination-mediated DSB signaling in OTUB2-depleted cells. Here, we noted that siRNA-mediated knockdown of OTUB2 affected only a small fraction of the total amount of ubiquitinated protein and the free ubiquitin pool (Figure S3A). First, we assessed whether OTUB2 depletion affected phosphorylation-mediated DDR signaling and excluded this possibility because OTUB2 siRNA-transfected cells and control siRNA-transfected cells showed similarly weak staining of γH2AX and MDC1 foci 5 min post-NCS treatment but then exhibited similarly strong staining for both foci 10 min post-NCS treatment (Figures

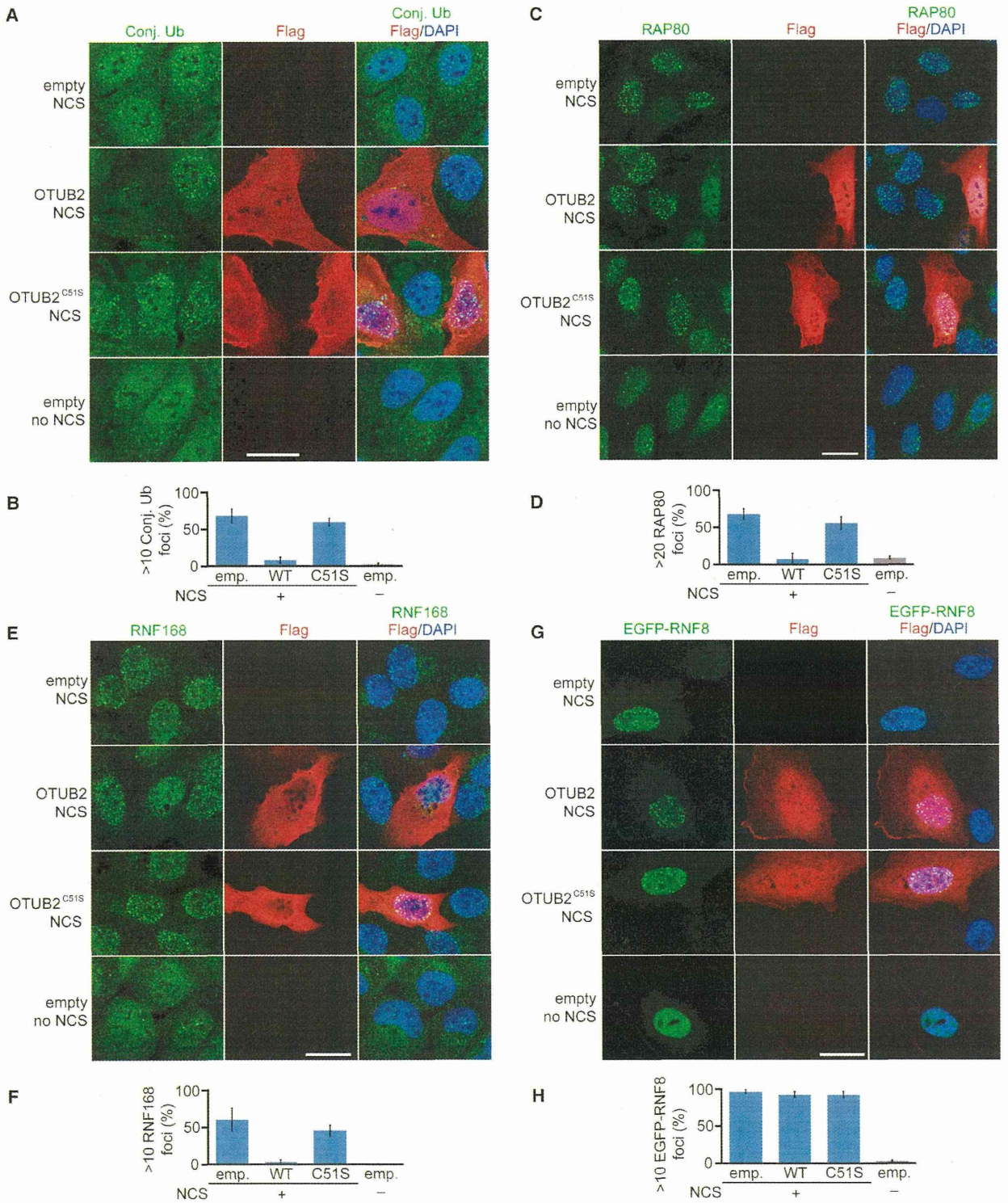

Figure 2. OTUB2 Negatively Regulates RNF8-Dependent DDR

(A–H) In (A), (C), (E), and (G), U2OS cells were transfected with Flag-OTUB2 or Flag-OTUB2^{C51S} expression plasmids. EGFP-RNF8^{C403S} and Flag-OTUB2 expression plasmids were cotransfected in (G). The cells were treated with 5 ng/mL NCS and processed for the indicated protein and Flag immunofluorescence

(legend continued on next page)

S3B and S3C). As observed in the siRNA screen, the assembly of RAP80 was enhanced in OTUB2-depleted cells (Figures 3A and 3B) but not in OTUB1-depleted cells 5 min post-NCS treatment (Figure S3D). Soon after the transient convulsive enhancement of RAP80 assembly, the percentage of OTUB2-depleted cells with RAP80 foci decreased and reached a similar level to that of the control cells 60 min post-NCS treatment (Figures 3A and 3B). Next, we examined ubiquitin conjugation at DSBs based on staining with an anti-conjugated ubiquitin (FK2) antibody. Control cells showed a gradual increase in the number of conjugated ubiquitin foci-positive cells during NCS treatment. In contrast, OTUB2-depleted cells exhibited many strongly staining foci 5 or 10 min post-NCS treatment (Figures 3C and 3D). In addition, OTUB2-depleted cells showed a higher frequency of RNF168 foci formation than control cells 5 or 10 min post-NCS treatment (Figures 3E and 3F). While ubiquitin conjugation was accelerated in OTUB2-depleted cells in an early phase of the DDR, the dissolution kinetics of the conjugated ubiquitin foci in the OTUB2-depleted cells were faster than those of control cells (Figures 3G and 3H). These data suggest that OTUB2 predominantly works during an early phase of the DDR but is not required for conjugated ubiquitin clearance in a later phase of the DDR. The faster conjugated ubiquitin clearance in OTUB2-depleted cells also suggests that DNA repair is accelerated in OTUB2-depleted cells. In contrast, OTUB1-depleted cells showed persistent conjugated ubiquitin foci as we previously reported (Nakada et al., 2010). Codepletion of OTUB2 and OTUB1 resulted in partial persistence of conjugated ubiquitin foci (Figures 3G, 3H, and S3E). These data indicate that OTUB2 and OTUB1 work during different phases of the DDR.

Next, we analyzed 53BP1 accumulation at DSBs. When control siRNA-transfected U2OS cells were treated with NCS, weakly stained, fine 53BP1 foci were predominant until 30 min after NCS treatment (Figures 4A and 4B). In contrast, the OTUB2-depleted cells exhibited larger and more strongly stained 53BP1 foci 20–30 min post-NCS treatment (Figures 4A and 4B). By 1–2 hr post-NCS treatment, most of the control cells and the OTUB2-depleted cells contained large 53BP1 foci (Figures S4A and S4B), indicating that 53BP1 accumulation was accelerated in the OTUB2-depleted cells. When an siRNA-resistant version of OTUB2 was weakly expressed in cells transfected with OTUB2-specific siRNA, the enlargement of 53BP1 foci was suppressed 20 min post-NCS treatment. However, this suppression did not occur when OTUB2^{C51S} was expressed in OTUB2-depleted cells (Figures 4C, S4C, and S4D). Therefore, we excluded the off-target effects of the siRNA and confirmed that OTUB2 indeed suppressed the DDR in a DUB activity-dependent manner. The enhancement of 53BP1 foci formation during an early phase of the DDR in OTUB2-depleted cells was completely abrogated when cells were simultaneously depleted of RNF8 or RNF168, indicating that OTUB2 acted on the RNF8/RNF168 pathway (Figures 4D, S4E, and S4F).

When we compared the assembly kinetics of RAP80 and 53BP1 foci formation, we observed that the accumulation of 53BP1 at DSB sites was slower than that of RAP80 (Figures 3B and 4B). Indeed, double immunofluorescence staining revealed that the majority of the RAP80 foci did not accompany the 53BP1 foci 5 min post-NCS treatment, although most of the foci colocalized with the 53BP1 foci 1 hr post-NCS treatment in OTUB2-depleted cells (Figure 4E). These data suggest that the accumulation of 53BP1 at DSB sites requires other signaling events that are not necessary for RAP80 foci formation, and this process is regulated by OTUB2.

OTUB2 Suppresses the Ubiquitination of L3MBTL1

We next sought to identify the targets of OTUB2. A recent study revealed that the recruitment of 53BP1 requires the RNF8-mediated ubiquitination-dependent removal of L3MBTL1 from damaged chromatin (Acs et al., 2011). Overexpression of Flag-L3MBTL1 more efficiently suppressed large 53BP1 foci formation than Flag-L3MBTL1$^{\Delta MBT}$, which lacked three MBT domains important for interaction with nucleosomes (Trojer et al., 2007) (Figures 4F and 4G), indicating that L3MBTL1 competes with 53BP1 for localization at DSBs. U2OS cells stably expressing L3MBTL1-specific shRNA more frequently showed large 53BP1 foci than nontargeting control shRNA-expressing cells 20 min post-NCS treatment in the presence of OTUB2, while RAP80 foci formation was not enhanced in shL3MBTL1-expressing cells (Figures S4G–S4K). In contrast, when OTUB2 was depleted by siRNA, control shRNA-expressing cells and L3MBTL1-specific shRNA-expressing cells exhibited similar frequencies of cells with large 53BP1 foci (Figures S4H, S4I, and S4K). These data suggest that OTUB2 is epistatic to L3MBTL1. Therefore, we focused on L3MBTL1 and asked whether OTUB2 prevented RNF8-mediated ubiquitination of L3MBTL1.

First, to confirm whether OTUB2 interacts with L3MBTL1, we performed a coimmunoprecipitation assay. Exogenously expressed Myc-OTUB2 was reciprocally coimmunoprecipitated with Flag-L3MBTL1 from U2OS cells (Figure 5A). Furthermore, endogenous OTUB2 was coimmunoprecipitated with Flag-L3MBTL1 from U2OS cells stably expressing Flag-L3MBTL1, and this interaction was independent of NCS treatment (Figure 5B). These data suggest that the interaction between OTUB2 and L3MBTL1 is constitutive rather than DNA damage dependent.

Next, we investigated whether OTUB2 could deubiquitinate L3MBTL1 in vivo. U2OS cells were transfected with His-L3MBTL1, HA-RNF8, and Myc-ubiquitin expression vectors and subjected to His pull downs under denaturing conditions. Overexpression of RNF8 successfully ubiquitinated His-L3MBTL1 (Figure 5C). Unexpectedly, all K/R ubiquitin mutants, in which one of seven Lys residues in ubiquitin was substituted with Arg, and a K0 ubiquitin mutant, in which all Lys residues

staining 1 hr after NCS treatment. The DNA was counterstained with DAPI. Representative images of the immunofluorescence staining are shown. Scale bar, 25 μm. In (B), (D), (F), and (H), the percentage of cells containing > 10 or >20 indicated protein foci was determined by counting 100 cells from the Flag-OTUB2-transfected cultures with strong fusion protein expression or 100 cells from the control cultures transfected with the Flag-empty plasmid from each sample. Data are presented as the mean ± SD of three independent experiments. emp., empty plasmid. See also Figure S2.

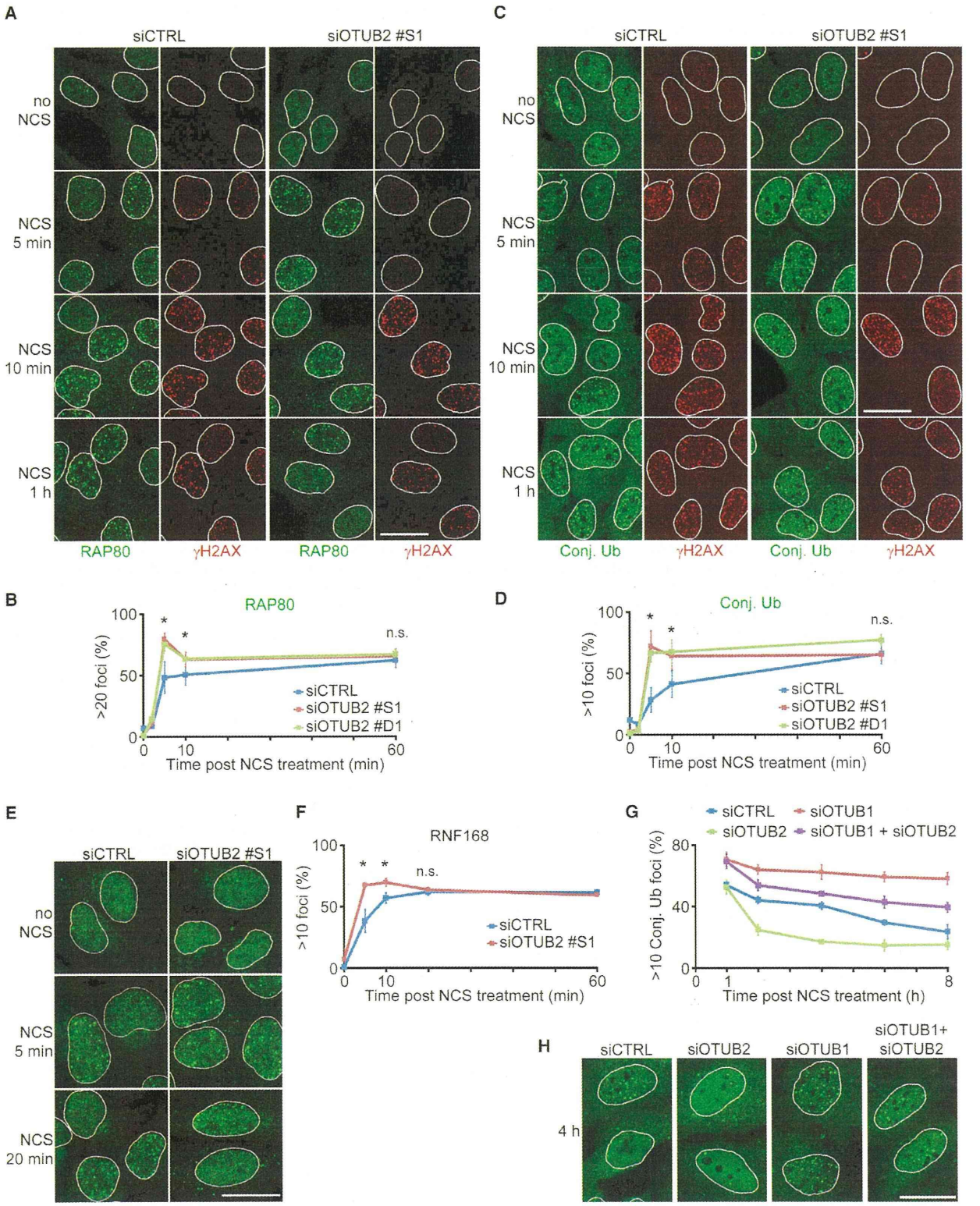

(legend on next page)